PTEP

Prog. Theor. Exp. Phys. **2017**, 12A107 (19 pages)
DOI: 10.1093/ptep/ptx169

Origin of Ultra High Energy Cosmic Rays

Observation of ultra high energy cosmic rays from space: Status and perspectives

M. Casolino[1,2,*], P. Klimov[3], and L. Piotrowski[2]

[1]*INFN, Structure of Rome Tor Vergata, Department of Physics, University of Rome Tor Vergata, Via della Ricerca Scientifica 1, 00133 Rome, Italy*
[2]*RIKEN, Global Research Cluster, 2-1 Hirosawa, Wako-shi, Saitama, 351-0198, Japan*
[3]*Skobeltsyn Institute of Nuclear Physics of Lomonosov Moscow State University, 1-2, Leninskie gory, GSP-1, Moscow 119991, Russian Federation*
[*]E-mail: casolino@roma2.infn.it

Received April 12, 2017; Revised November 6, 2017; Accepted November 7, 2017; Published December 29, 2017

The study of ultra high energy cosmic rays (UHECRs) offers unique possibilities to probe the energies currently inaccessible by man-made accelerators. Recent years have shed light on several characteristics of these particles, but—due to their extremely low flux—their origin, nature, and acceleration mechanisms are still unclear. Space-based observations have the potential for an increase in statistics, up to several orders of magnitude, and would be able to cover the whole sky, allowing for a direct comparison of spectra and direction of arrival. A detector with the exposure of a few times that of the Pierre Auger Observatory would be able to clarify the observed differences between the northern and southern skies, confirm the existence of TA hot spot, and measure multipolar anisotropies with high precision. A number of novel technologies—from optics to sensors, front-end and read-out electronics—have been developed over the years to achieve this goal. In this paper we describe the progress and results obtained so far and discuss the perspectives of UHECR physics observation from space.

Subject Index F00, F03

1. Introduction

Ultra high energy cosmic rays (UHECRs) allow phenomena occurring at energies currently inaccessible by man-made accelerators to be studied. Although recent years have shed light on several characteristics of these particles with $E > 10^{18}$ eV, their origin, nature, and acceleration mechanisms are still unclear. A more detailed understanding of UHECR can shed light on the highest energy astrophysics and particle physics mechanisms, potentially addressing yet-unknown phenomena, such as Big Bang cosmology or Lorentz invariance violation. The difficulty in unraveling these problems lies in the extremely low flux of particles above 5×10^{19} eV, which requires the construction of very large ground-based detectors, such as the Pierre Auger Observatory (PAO) in the southern hemisphere and the Telescope Array (TA) in the northern hemisphere. However, the restriction of statistics still limits the results of these arrays, which also observe two different portions of the sky, making a comparison of the results more difficult. Space-based observations have the potential for an increase in statistics, up to several orders of magnitude, and would be able to cover the whole sky uniformly, allowing for a direct comparison of spectra and direction of arrival on the celestial sphere.

J. Linsley and R. Benson (Ref. [1]) were the first to propose the fluorescent registration of Extensive Air Showers (EAS) using a UV telescope on board a satellite. This idea has been developed in

a number of projects. In the USA there were the proposals of OWL-AIRWATCH (Refs. [2–4]), and in Europe the first EUSO (ESA) design (Refs. [5,6]). In parallel, in Russia, detectors that use concentrator mirrors for collecting fluorescence light (TUS and KLYPVE) were proposed and developed (Refs. [7,8]) with TUS, the first orbital detector of UHECRs, being launched aboard the Lomonosov satellite on 28 April 2016 (see below).

2. The EUSO program

The aim of the JEM-EUSO program (Fig. 1) is to bring the study of UHECR to space (Ref. [9]). The principle of observation is based on the detection of UV light emitted by isotropic fluorescence of atmospheric nitrogen excited by the EASs in the Earth's atmosphere and forward-beamed Cherenkov radiation reflected from the Earth's surface or dense cloud tops.

A space-based detector for UHECR research has the advantage of a much larger exposure and a uniform coverage of the celestial sphere. The design of a space-based telescope for UHECR observation has strong constraints on power, mass, size, and data transmission bandwidth and requires the development of a number of novel technologies, from optics to sensors, front-end and read-out electronics.

In this work we describe the current and future pathfinders and missions that employ and test the principles of observation and technology of any EUSO-type mission: (a) a ground-based detector (EUSO-TA) operating on the TA site in Utah; (b) EUSO-BALLOON, a stratospheric flight successfully carried out in 2014 from Timmins, Canada; (c) EUSO-SPB, a NASA ultra-long-duration balloon flight (12 days) from New Zealand (2017); (d) Mini-EUSO, to observe the Earth through a UV transparent window inside the ISS (2018); (e) K-EUSO, the first reflector telescope with size

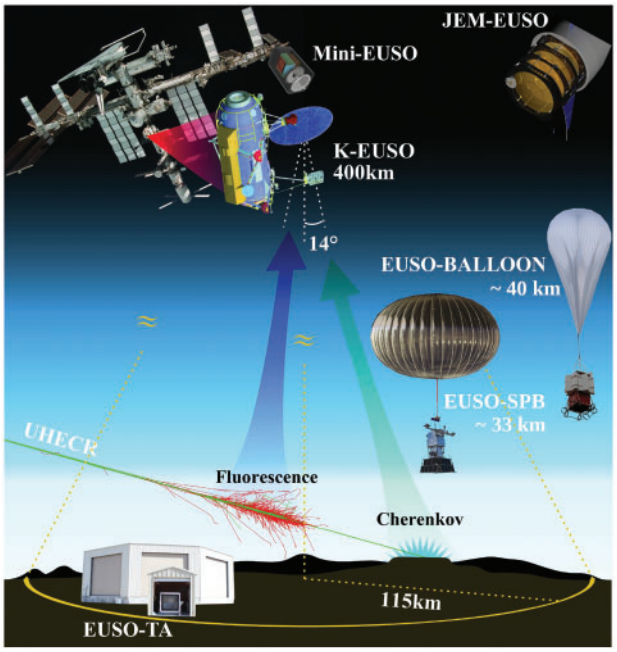

Fig. 1. The detectors of the JEM-EUSO program: (a) EUSO-TA: Ground detector installed in 2013 at the TA site; (b) EUSO-BALLOON: First balloon flight from Canada, August 2014; EUSO-SPB: Long duration NASA flight, New Zealand, 2017, 2022; (c) Mini-EUSO: Earth observation telescope to be installed inside the International Space Station (ISS) in 2018; (d) K-EUSO (2022): Reflector telescope to be installed on the Russian section of the ISS; (e) Large-size telescope (JEM-EUSO / POEMMA > 2025).

and resolution capable of carrying out UHECR science from space in 2022; (f) JEM-EUSO, a large field of view refractor telescope designed to have at least 10 times the acceptance of PAO (Ref. [10]).

3. EUSO-TA

EUSO-TA is a ground-based detector located at the TA site in Black Rock Mesa, Utah, USA (Fig. 2). The telescope can perform observations of UV light generated by cosmic-ray-induced EASs and stars, as well as from artificial sources such as lasers. The aim of the project is to study the detector response to cosmic rays in conjunction with the TA fluorescence detector (TAFD).

The EUSO-TA detector consists of two 1 m^2 Fresnel lenses with a field of view of $10.6° \times 10.6°$ (Fig. 3). Light is focused onto the photo detector module (PDM), composed of 36 Hamamatsu multi-anode photomultipliers (64 channels per tube), for a total of 2304 channels (see Fig. 4, bottom left). Front-end readout is performed by 36 application specific integrated circuits (ASICs), with trigger and further readout tasks performed by two acquisition boards that send the data to a CPU and storage system. The telescope is housed in a shed located in front of one of the TAFDs, pointing in the direction of the electron light source (ELS) and the central laser facility (CLF). The PDM structure and readout scheme is identical to the ones employed for the other telescopes of the EUSO program.

Measurements of the UV background in different darkness conditions, moon phases, and instrument inclinations have been completed, as well as observations of various stars of different magnitude

Fig. 2. EUSO-TA (front right), the main detector of the EUSO-SPB (front left) and the TA fluorescence detector (back) (picture by M. Mustafa).

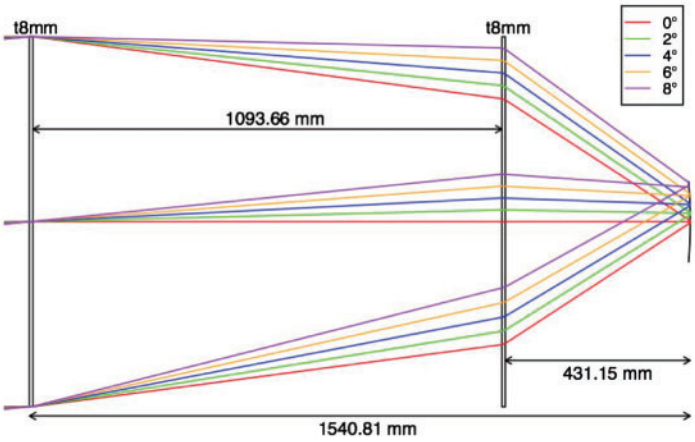

Fig. 3. EUSO-TA optics design. Light enters at the left of the picture and is focused by the two Fresnel lenses (1 m^2) on the photo detector module on the right.

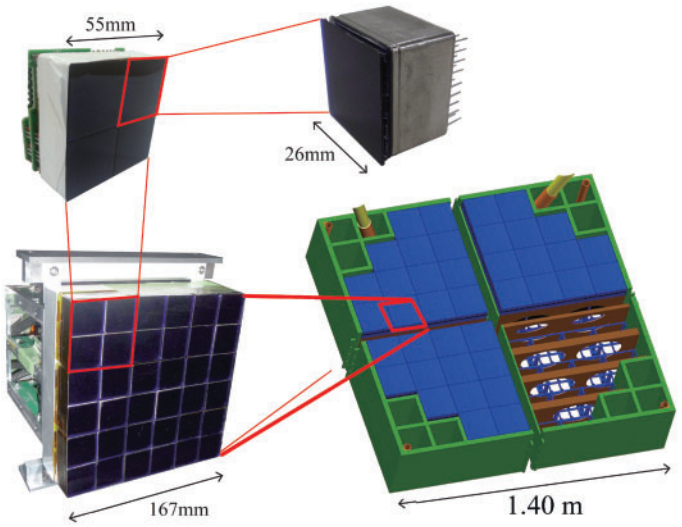

Fig. 4. Top right: One Hamamatsu multi-anode photomultiplier (MAPMT) with 64 channels. Four of these are joined in an elementary cell (EC) unit which shares the high-voltage power supply and the cabling (top left). The PDM consists of 36 MAPMTs, for a total of 2304 pixels (bottom left). Bottom right: Structure of the 52 PDM focal surface (FS) of the K-EUSO FS. In the K-EUSO-Schmidt optics, the FS is curved.

and color index. Subsequently, cosmic ray events ($E \geq 10^{18}$ eV)—triggered by TA—have also been observed. In September 2015, the self-trigger algorithm used in EUSO-SPB was tested. Current work aims to increase the field of view of the detector with the addition of a second PDM and to improve the statistics of cosmic-ray events.

3.1. Stars and the point spread function

Preliminary analysis shows that EUSO-TA can observe stars up to $m_B \simeq 6.5$ on averages of 1280 frames. One frame is defined as a *gate time unit* (GTU) of duration of 2.5 μs each. The total averaging time is thus 3.2 ms. While very bright stars can be seen on single frames, stacking improves the signal-to-noise ratio, resulting in the observation of fainter objects. The stars can be used as point sources to study the point spread function (PSF) of our detector. Initial analysis performed with a fit of a standard Gaussian profile gives a PSF with average full width half maximum of 2.35 pixels, well within the requirements needed for detection of UHECR showers.

3.2. Laser light

The EUSO-TA response has been studied using the light coming from the TA CLF, situated about 21 km from EUSO-TA. The CLF shoots vertical laser pulses of 355 nm wavelength in front of the detectors (Ref. [11]). During standard observation nights, the CLF shoots every 30 minutes for 30 s with 10 Hz shooting frequency. The scattered light of the ~ 3 mJ beam was clearly observed traversing through the EUSO-TA field of view. Shots are visible on 6 to 8 frames, depending on the pulse initial position in the EUSO-TA field of view and acquisition time synchronization, each extending for a longitudinal length of 6–8 pixels, depending on the position on the frame, which is consistent with expectations. The intensity of the observed light is dependent on the atmospheric conditions, e.g., obstruction of the light path due to clouds. With a clear sky, the measured intensity spread is compatible with the fluctuations of the ejected laser beam intensity, showing the good reconstruction capabilities of EUSO-TA.

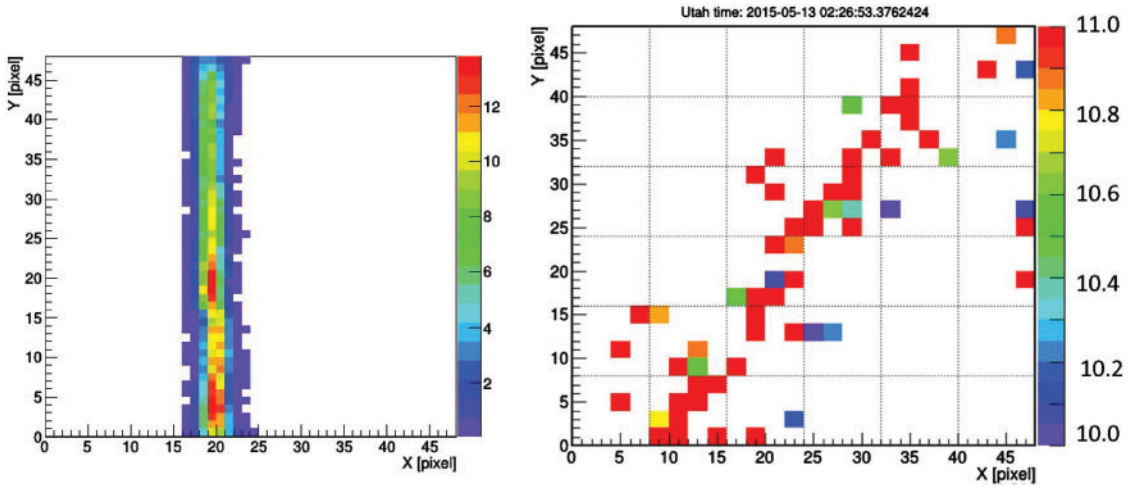

Fig. 5. Left: An average of ∼ 250 shots of a CLF laser. Right: A UHECR event of $\sim 10^{18}$ eV energy traversing at ∼ 2.5 km distance from EUSO-TA and therefore visible as a track on a single 2.5 μ*s* frame (1 GTU), in this case going from top right to bottom left (distance and energy are estimated by TA). The image is rebinned (2 × 2 pixels) and thresholded. The color scale denotes the raw number of detected counts (before calibration).

We have also performed measurements using a mobile global light system (GLS) UV laser from the Colorado School of Mines. The laser was shot with energies in the range of about 1–86 mJ, with pointing adjustable in two dimensions. The mechanics featured automatic changing of the pointing, allowing for easy "sweeps" through the field of view. EUSO-TA was able to detect a few shots of 1 mJ energy shot vertically from a distance of 34 km, suggesting that the sensitivity is better than expected.

Furthermore, the EUSO trigger foreseen for the EUSO-SPB has been tested in EUSO-TA, successfully triggering on CLF and GLS laser light.

3.3. Cosmic ray events

Several cosmic ray events have been observed. At the moment we have 9 candidates, all at a distance between 1.5 and 9 km and an energy $10^{17.7} \leq E \leq 10^{18.8}$ eV, a number consistent with expectations. The events have been triggered by TA, which sent the signal to EUSO-TA. Energy and distance reconstruction information are coming from TA. This can be used to calibrate our detector response and the related simulations. Given the proximity of the events and the sampling rate of 2.5 μs/GTU, the track usually goes through the whole field of view (FOV) in a single GTU, as shown in Fig. 5 (right).

4. The EUSO balloon flights

The balloon flights offer a unique possibility to develop the EUSO detectors and test the observation principle in similar conditions to those encountered in space. Actually, the residual atmosphere is a more demanding test of the high-voltage power supply system of the photomultiplier tubes (PMTs), since a discharge is more likely than in vacuum. Also, the limited telemetry from the balloon (since it is necessary to assume that the payload is not recovered) requires more stringent constraints to the trigger than in the case of a space-based detector. In the latter case, more bandwidth is generally available and—in the case of the ISS—data can be physically sent to the ground on hard disks.

4.1. EUSO-BALLOON

The EUSO-BALLOON flight took place in August 2014 from Timmins, Canada (Ref. [12]). The CNES (French Space Agency) balloon carried an instrument similar to EUSO-TA, pointed towards the nadir from a float altitude of about 40 km. The objective of the EUSO-BALLOON was to perform a full end-to-end test of all the main subsystems in a near-space environment. In this way it was possible to test the key technologies and methods featured in its future space mission and raise their technological readiness level (TRL).

The total mass of the payload was about 320 kg. The optical bench contained two Fresnel lenses made from 8 mm thick polymethyl methacrylate with a front surface of 100 × 100 cm each. The instrument booth was made as a watertight capsule using a front Fresnel lens as a porthole.[1] Besides the PDM and associated electronics, similar to the ones developed for the main mission, the instrument booth housed the telemetry system (SIREN), CNES specific instrumentation (ICDV, Hub), and two battery packs of 28 V—the same voltage that will be used on the ISS for JEM-EUSO. Ancillary payloads included an infrared camera, a visible light camera, and a Geiger particle counter. During the flight we were able to observe the Earth's albedo from different ground types (forest, town, lakes), as shown in Fig. 6 (top). Furthermore, a NASA-funded helicopter was following the balloon trajectory, generating artificial light using xenon lamps, and mimicking an EAS using a laser beam. Both the xenon flashes and the laser shots were successfully detected by the apparatus (Fig. 6, bottom). All systems worked correctly and according to specifications. The PDM was functioning for the whole time, and the high-voltage power supply was stable and operated with no trouble in the residual atmosphere of 40 km altitude.

4.2. EUSO-SPB

In 2017, EUSO-SPB flew from New Zealand for a long duration flight (Fig. 7) of 12 days. This flight employed NASA's new super pressure balloon (SPB) technology, which uses a sealed balloon to achieve circum-Antarctic flights with a duration of more than a month. The first technological test flight was successfully performed by NASA in 2015. The EUSO-SPB includes a new set of lenses with improved parameters and a new PDM with higher gain PMTs. Use of a new ASIC chip—SPACIROC 3—increases the saturation level from ∼ 30 to more than 150 photoelectrons. The experiment also houses two auxiliary devices: an infrared camera and a silicon photomultiplier-based detector with 256 pixels.

The long duration flight was devoted to detecting several EASs by looking downwards from an altitude of about 33 km. Its low elevation compared to JEM-EUSO (33 km vs. 400 km) and the lens size cause the balloon energy threshold for shower detection to be about 3×10^{18} eV. The field of view of about 11° × 11° results in ∼ 7 × 7 km instantaneous aperture on the ground and a spatial resolution better than 150 m.

EUSO-SPB optics and electronics have been extensively tested on-ground, including measurements performed at the TA site in Utah, along EUSO-TA. Observations of stars, CLF, and GLS lasers have been performed, as well as absolute calibration. The detector passed two hang and compatibility tests required by NASA. The detector flew for 12 days in April 2017 (Ref. [13]). A second SPB flight, EUSO-SPB2, is under preparation (Ref. [14]).

[1] This protected the electronics in the water landing, with the payload being successfully recovered.

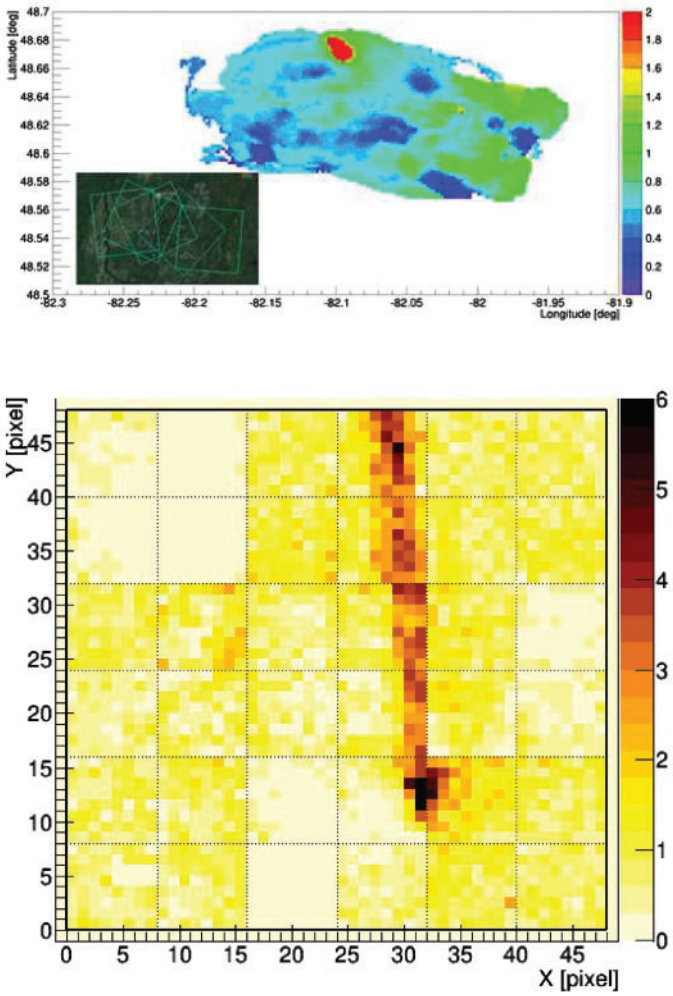

Fig. 6. Top: UV background map (arbitrary units) in the region of Timmins. The red spot at the top is the light from a mine. Bottom: Experimental data registered by the EUSO-BALLOON of a laser shot from a helicopter flying below the gondola. The picture is the sum of 9 frames (22.5 μs total time) during which the signal was moving from the bottom to the top. The color scale shows detector counts.

5. Mini-EUSO

The Mini-EUSO space experiment ("UV atmosphere" in the Russian space program) is designed to perform orbital observations in the UV spectrum, pointing towards Earth (Ref. [15]). Mini-EUSO presents the opportunity to study a diverse range of scientific subjects including atmospheric physics, strange quark matter, bioluminescence, and UHECRs. It will also create a high resolution, night-time map of the Earth in UV light. The mission is devised with the intention of raising the TRL of the future JEM-EUSO mission to observe UHECRs from space. The Mini-EUSO measurements will be performed from the ISS through a UV transparent window in the Russian Zvezda Service Module. Furthermore, Mini-EUSO is the first step in a roadmap of potential space debris removal via laser ablation (Ref. [16]).

The Mini-EUSO instrument (Fig. 8) comprises a compact telescope with a large field of view ($38° \times 38°$), based on an optical system employing two 25 cm-diameter Fresnel lenses (focal length $\simeq 30$ cm) for increased light collection. The UV light is focused onto one PDM module and stored on on-board disks. The observations will be performed on μs-to-second scales both in triggered modes

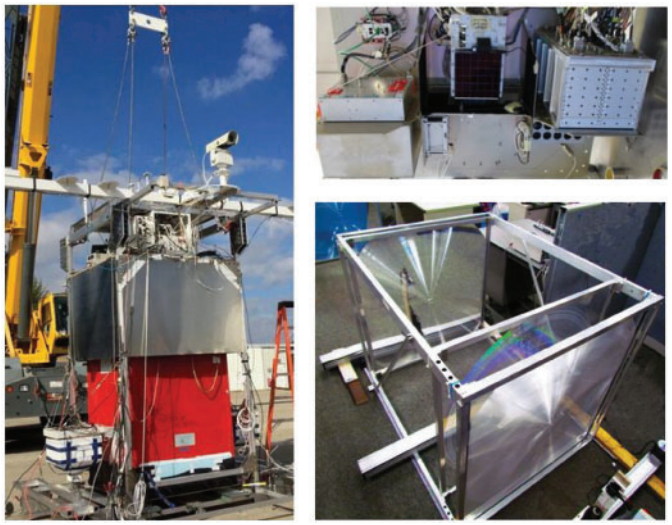

Fig. 7. Left: The EUSO-SPB payload in the flight configuration during stand-alone hang tests in Palestine, Texas. Top right: The electronics with the PDM focal surface in the center. Bottom right: The Fresnel lens optics.

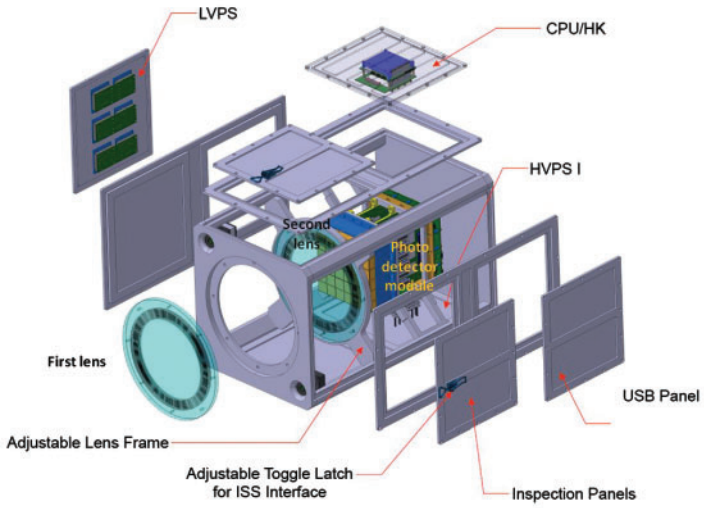

Fig. 8. Exploded view of the Mini-EUSO detector. Dimensions are 35 × 35 × 60 cm (lens diameter 25 cm).

(separately for fast and slow events) and "film mode" consisting of data taken at regular intervals. Launch is foreseen by winter 2018 with operations lasting at least three years.

6. Moscow State University space-based experiments for UV background studies

Since 2005, the Skobeltsyn Institute of Nuclear Physics of Moscow State University (MSU) has made a series of experiments aimed at studying the UV radiation of the night atmosphere to estimate the background and source of false triggers for UHECR detectors. This study was carried out by the simple UV detectors (DUV) installed on board the Universitetsky-Tatiana (Tatiana-1) (Ref. [17]), Universitetsky-Tatiana-2 (Tatiana-2) (Ref. [18]), and Vernov (Ref. [19]) satellites (Fig. 9) looking in the nadir direction. The DUV contains two Hamamatsu R1463 PMTs with multi-alkali cathodes, covered by filters (UV and IR). In the UV part of the detector, the filter UFS1 is transparent to

Fig. 9. MSU satellites equipped with UV detectors. From the left: Tatiana-1, Tatiana-2, Vernov.

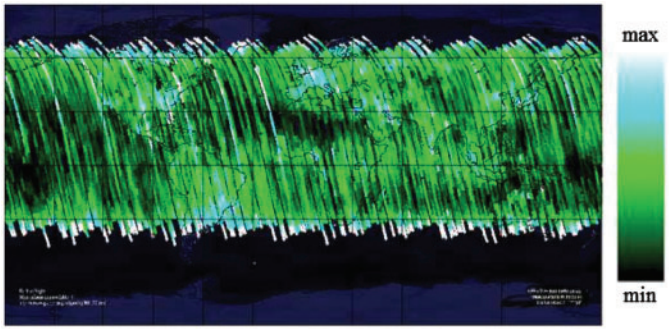

Fig. 10. The map of UV atmospheric radiation during moonless nights measured by the Tatiana-2 experiment (arbitrary units).

wavelengths in the 240–420 nm range. The quantum efficiency of the PMT's cathode in the UV region is $\sim 20\%$. The field of view of the detectors is restricted by a collimator. The area of the PMT cathode effective for detecting photons changes between 0.4 cm^2 for 0° from the detector's optical axis, to 0 cm^2 for 20°. The overall geometry factor of the DUV is 0.024 cm^2 sr. These detectors are similar in all experiments, but differ in temporal resolution (16 μs and 64 μs for Tatiana-1, 1 ms for Tatiana-2, and 0.5 ms for Vernov). The main feature of data acquisition was the usage of an automatic PMT gain control system (GCS). GCS establishes feedback between UV intensity measurements with an analogue-to-digital converter (ADC) and a dedicated digital-to-analog converter (DAC), which is controlling voltage on a PMT. This allows measurements of a variable UV background to be conducted without switching off the equipment. Measurements of high-voltage power supply of PMTs and ADC code of digital oscillograms provide monitoring of slow UV variations along the satellite trace and detection of transient atmospheric events (TAEs).

During moonless nights, the measured atmospheric UV radiation was $3–5 \times 10^7$ ph cm^{-2} s^{-1} sr^{-1} and a general increase of UV intensity was observed over all regions of the atmosphere on moonlit nights. On a full-moon night it was up to 2×10^9 ph cm^{-2} s^{-1} sr^{-1} in cloudless areas and 4×10^9 ph cm^{-2} s^{-1} sr^{-1} over clouds, with the highest UV intensities of the order of 10^{10}–10^{12} ph cm^{-2} s^{-1} sr^{-1}. The results of all experiments are in agreement with each other, showing several districts with the lowest UV intensity: (1) deserts, such as the Sahara; (2) parts of the Pacific Ocean; (3) parts of Siberia. The map obtained by the Tatiana-2 experiment is shown in Fig. 10. The impact of anthropogenic sources was estimated to be about 2×10^8 ph cm^{-2} s^{-1} sr^{-1}.

A number of various types of TAE, mostly related to thunderstorm activity, were measured. During 166.5 hours of operation of the Vernov satellite, more than 8500 TAEs were registered. These events were classified by their temporal structure and UV radiation intensity. Examples of events are shown

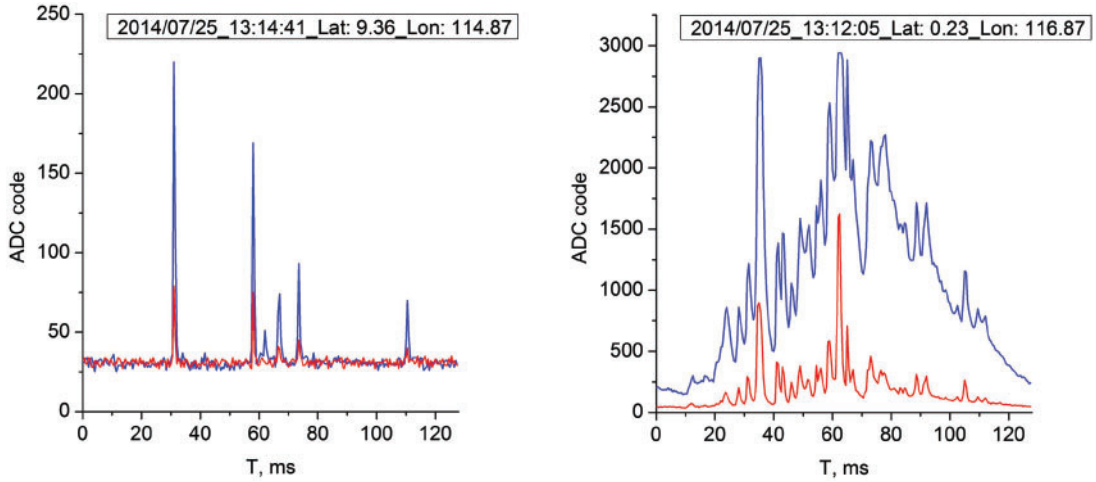

Fig. 11. Examples of transient atmospheric events measured by the Vernov satellite. Blue: UV channel (300–400 nm); Red: Red–IR channel (600–800 nm).

in Fig. 11. The number of photons released in the atmosphere (Q_a) during these phenomena is 10^{20}–10^{26}. Tatiana-2 found that dim flashes ($Q_a < 10^{23}$) have a more uniform geographical distribution, while bright ones are concentrated in well-known thunderstorm regions (Ref. [20]). Dim and short flashes can imitate UHECR events and produce a large number of false triggers (Ref. [21]). The rate of TAEs to be measured by K-EUSO and JEM-EUSO detectors was estimated in Ref. [22] based on the data from the Tatiana-2 experiment.

A joint analysis of transient atmospheric events measured by Vernov and a World Wide Lightning Location Network (WWLLN, http://wwlln.net/) has shown that nearly 80% of flashes occur in thunderstorm regions. At the same time, a number of TAEs measured in high latitudes far from active thunderstorm regions (presumably not associated with lightning) were separated from all TAEs. Their features are discussed in Ref. [23].

It is interesting that a huge number of events are grouped in series (consecutive measurements of 3 or more TAEs; Ref. [20]). The geographical distribution of the transient series is strongly correlated with the active thunderstorm regions in Tatiana-2 and Vernov experiments. On the other hand, TAEs that are "not serial" can be seen outside active thunderstorm regions. A duration of the series up to 15 minutes indicates a large region of thunderstorms—up to 1000 km—with a huge number of flashes with different time intervals (from milliseconds to seconds).

7. The TUS detector on board the Lomonosov satellite

The TUS detector is the first attempt to measure UHECR fluorescent light from space. It was launched on 28 April 2016, on a polar sun-synchronous orbit with an inclination of 97.3°, a period of ∼ 94 min, and an altitude of about 500 km. The TUS detector consists of two main parts: a parabolic mirror-concentrator of the Fresnel type and a square-shaped 256-pixel photodetector in the focal plane of the mirror. The mirror has an area of about 2 m^2 with a focal distance of 1.5 m. A pixel field of view equals 10 mrad, which results in a spatial resolution of 5 km, and an overall TUS FOV of approximately 80 × 80 km at sea level. Each pixel of the TUS photodetector is a Hamamatsu R1463 photomultiplier tube (the same as for the Tatiana and Vernov experiments). Light guides with square entrance apertures (15 × 15 mm) and circular outputs were employed to fill uniformly the

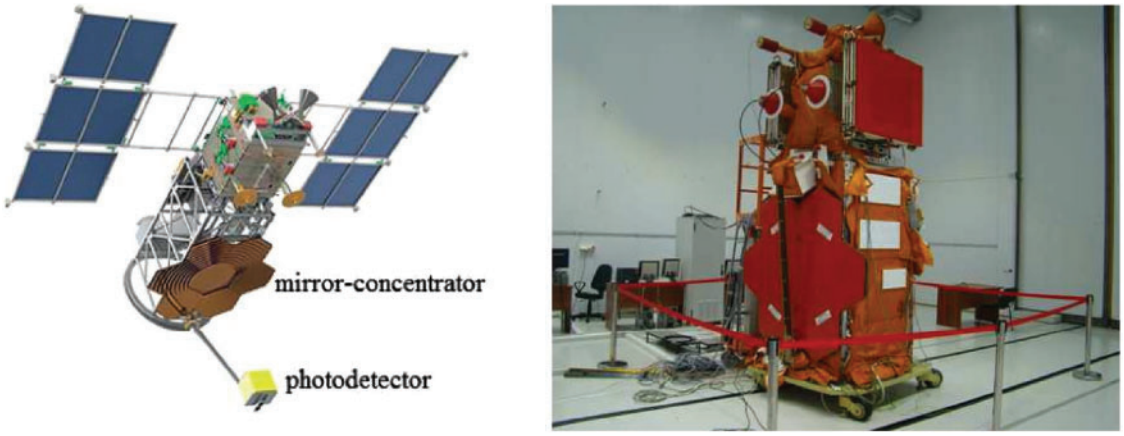

Fig. 12. Artist's view of the TUS detector on board the Lomonosov satellite (left). The TUS on board the Lomonosov satellite covered with a protective cover during preflight preparations at the Vostochny Cosmodrome (right).

detector's FOV. Each pixel has a black blind 1 cm above the light guide to protect it from stray light. A UV filter of 13 mm diameter and 2.5 mm thickness is placed in front of each PMT. The pixels are grouped in 16 identical photodetector modules. Each cluster has its own digital data processing system for the first-level trigger, based on a Xilinx Field-Programmable Gate Array (FPGA), and a high-voltage power supply controlled by the FPGA. The central processor board gathers information from all modules, controls their operation, and implements the second-level trigger algorithm. The TUS electronics can operate in four modes intended for detecting various fast optical phenomena in the atmosphere at different timescales with different time sampling. The main mode is aimed at registering UHECR and has a time sampling of 0.8 μs. This mode is also efficient for short TAE measurements of, e.g., elves. Slower modes have time sampling of 25.6 μs, 0.4 ms (for studying TAEs of different kinds that are slower than elves: e.g., sprites, blue jets, gigantic jets). An even slower mode of 6.6 ms is devoted to the detection of micro-meteors, space debris, and thunderstorm activity at a longer timescale. Waveforms in each mode consist of 256 time samples. The trigger algorithm consists of two levels. The first-level trigger decision is based on a comparison of the simple moving average of ADC counts calculated for each pixel with a threshold level that depends on the mean value of the background noise. At the second-level trigger, the geometry and number of pixels hit are analyzed. In the case of EAS and meteors, it is a search for a track, i.e., adjacent pixels lined up within a certain time.

The TUS on board the Lomonosov satellite and during preflight preparations at the Vostochny Cosmodrome is shown in Fig. 12.

During the first months of operation, the TUS detector measured numerous UV transient flashes in the EAS mode with different temporal dynamics and spatial structure. The most common type of TAE with a specific geometry of the development in the ionosphere is elves—the result of the ionosphere heating by an expanding electromagnetic wave from a powerful cloud-to-ground lightning (Ref. [24]). One of them was registered on 18 September 2016 (Fig. 13). The arc-like shape of the track made by the brightest PMTs and the speed of development support the hypothesis that this was an elve.

Another type of event consists of ADC counts monotonically increasing over ~ 100 μs. Such a flash typically evolves simultaneously in a majority of pixels presenting an almost uniform illumination

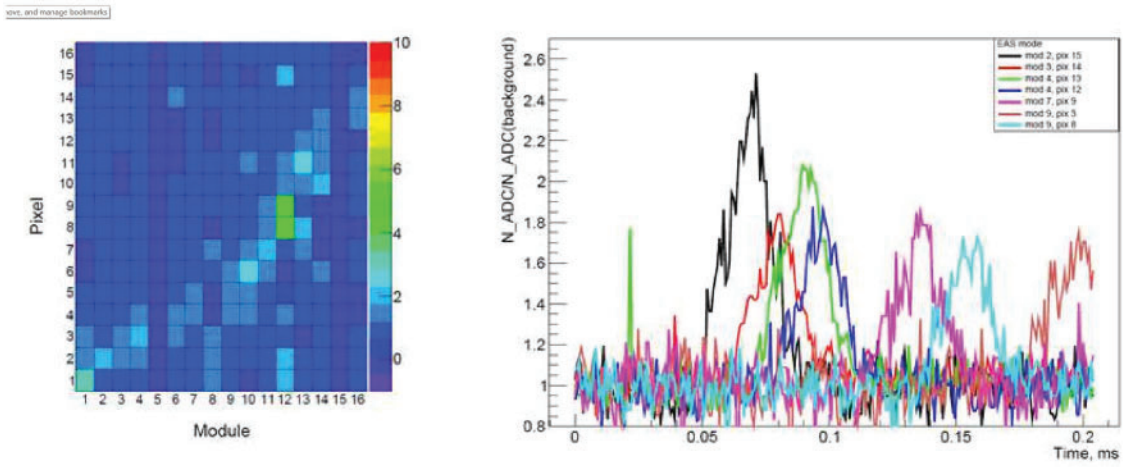

Fig. 13. Left: Snapshot of the focal plane which shows the arc-like shape of the elve in the TUS FOV. The snapshot was taken at $t = 0.174$ ms from the beginning of the record. Colors denote the signal amplitude in arbitrary units scaled to individual PMT gains. Right: Waveforms of several hit pixels. The Y-axis is a ratio of ADC counts and background signal for each pixel.

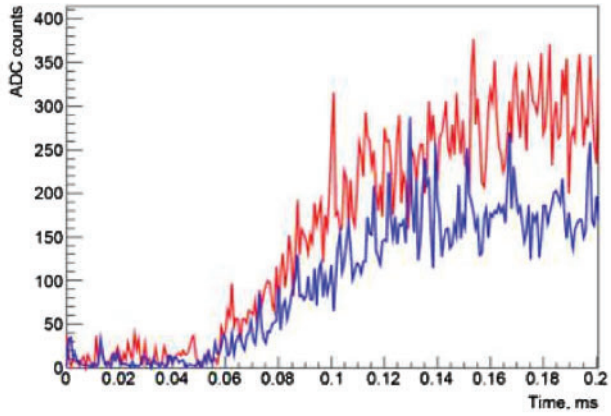

Fig. 14. Example of a "monotonic" flash waveform in two pixels.

of the focal plane. An example of such a waveform is shown in Fig. 14. In most cases, the global maximum of a flash is not passed prior to the end of the recorded trace (200 μs).

A comparison of TUS data for this type of event with WWLLN and Vaisala GLD360 (Ref. [25]) networks shows that they are related to thunderstorm activity, but the majority of lightning that can produce this signal on the whole focal plane of the detector occurs outside the TUS FOV (Ref. [26]). The reason for this effect is that the TUS mirror has two components of reflection: a focusing part, which produces the image of the event, and a diffuse part due to the scattering on the mirror roughness. The diffuse scattering part of the mirror has a much wider FOV than the focusing part, and the probability of lightning detection (or transient events related to them) outside the actual FOV is higher. This is an important result that shows the advantage of the Schmidt design of the K-EUSO detector, which more efficiently protects from stray light.

One more unexpected type of event that was measured by TUS in EAS mode is instant (i.e., happening in one or, rarely, two time samples of 0.8 μs) intensive flashes that produce tracks or, sometimes, small spots in the focal surface. They are likely to be caused by direct hits of low-energy

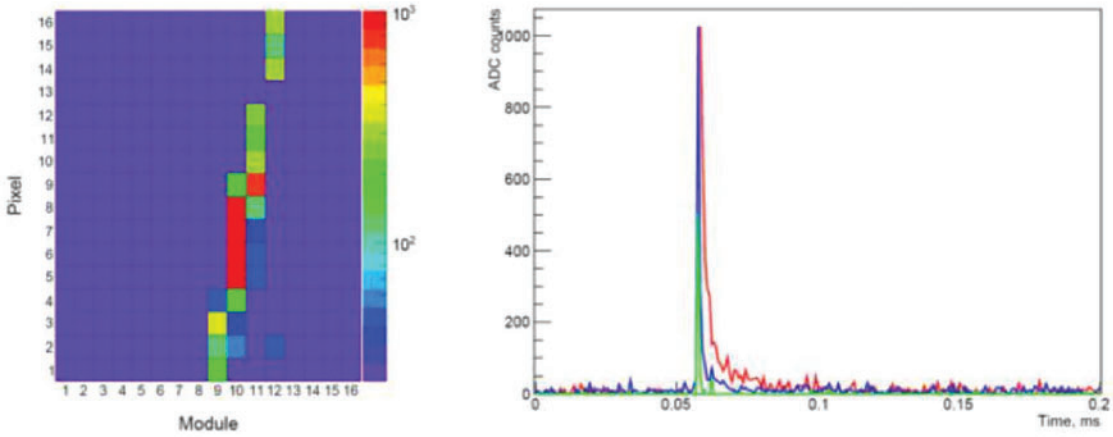

Fig. 15. Instant intensive flash registered on 25 October 2016. Left: Snapshot of the focal surface at the moment of maximum ADC counts. Right: Waveforms of 10 PMTs that demonstrated the biggest ADC counts. Colors denote different pixels.

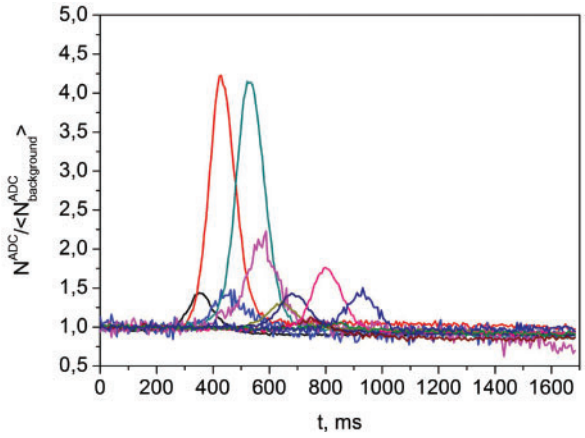

Fig. 16. Example of meteor waveforms measured by the TUS detector on 3 January 2017. Colors denote different pixels.

cosmic ray particles. These events and the results of their simulation in GEANT4 are described in Ref. [27]. An example of a track-like event is shown in Fig. 15. One can see a flash that occurs during one frame simultaneously in a group of PMTs lined up in a track. These events comprise approximately 14% of all measurements and a special trigger modification during the TUS flight was developed to suppress the rate of their registration. This should be considered in detail and taken into account during preparation of the new missions (K-EUSO, JEM-EUSO).

With such a varied noise, the search for real EAS events is currently in progress. But due to a high threshold of the TUS detector, EAS is expected to be a very rare event. It is important to note that an orbital UHECR detector can measure a variety of phenomena of different origins and represents the real multi-functional orbital laboratory for the low atmosphere, ionosphere, near-Earth environment, solar–terrestrial connections, meteors, and particle astrophysics studies. As an additional example of the orbital detector capabilities, we show the meteor waveform measured by the TUS detector (Fig. 16).

8. K-EUSO

K-EUSO continues the Russian program for UHECR studies from space by employing the technology developed in EUSO telescopes to achieve a large and uniform exposure over the whole sky (Fig. 17). It will be the first detector with a real capability for the UHECR spectrum and anisotropy study and the full celestial sphere coverage (Ref. [28]). Since its first conception as KLYPVE, the K-EUSO project has passed various modifications aimed at increasing FOV and UHECR statistics (Refs. [30–32]).

The recently adopted optical layout is a Schmidt camera covering a field of view of 40° with an entrance pupil diameter of 2.5 m, a 4 m-diameter spherical mirror and a focal length of 1.7 m (Fig. 18). The number of expected events to study anisotropy and dipole presented below refers to this configuration.

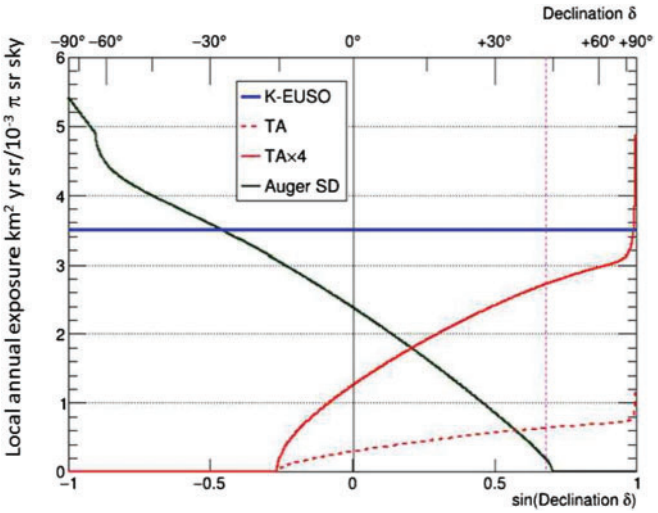

Fig. 17. Differential annual exposures for K-EUSO, TA, TA × 4, and PAO. It is possible to see the flat response of K-EUSO (K-EUSO-Schmidt is three times K-EUSO) compared with the ground detectors (see Refs. [28,29] for the estimation of the efficiency and effect of clouds).

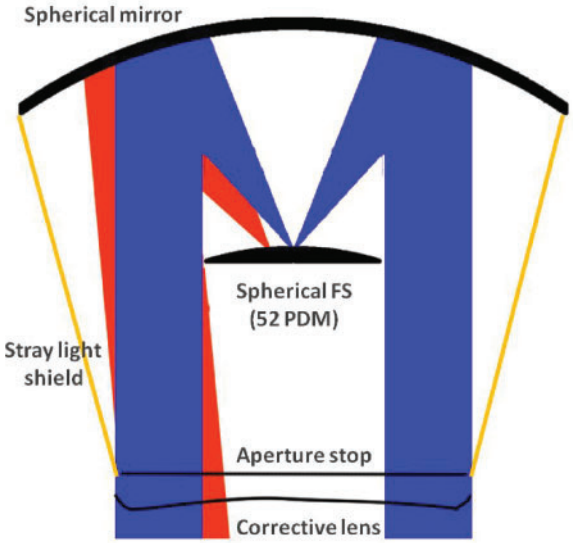

Fig. 18. Scheme of K-EUSO-Schmidt optics, with the spherical reflector (4 m diameter) on top and the corrective lens and spherical focal surface on the bottom.

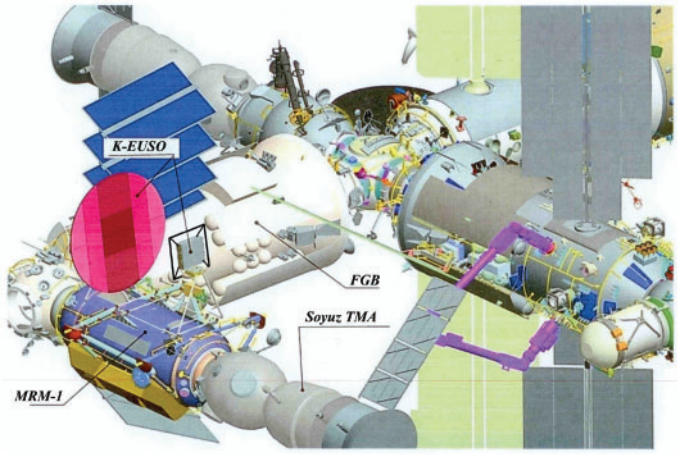

Fig. 19. Location of K-EUSO on the MRM-1 module of the Russian section of the ISS.

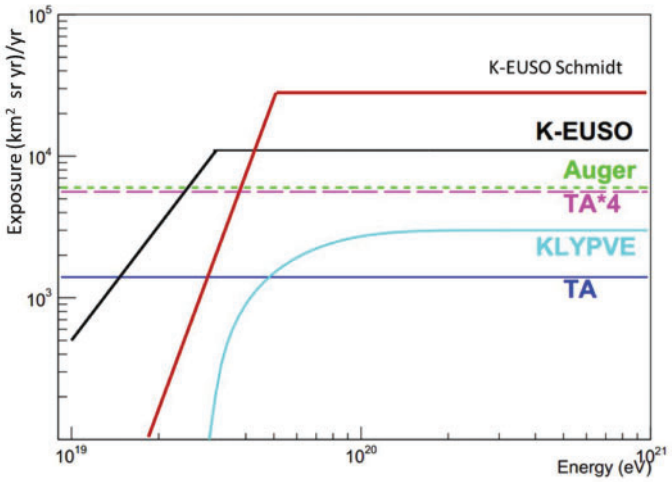

Fig. 20. Comparison of the exposures of the various ground-based and space-borne detectors. K-EUSO-Schmidt optics offers a higher exposure at higher energies. Note that the minimum energy threshold in the Schmidt optics is increased due to the larger shadow of the focal surface.

The temporal and spatial evolution of UV light recorded by K-EUSO will allow the energy and arrival direction of the UHECR to be determined. The camera focal plane is covered by 1.2×10^5 pixels, each smaller than 2.88×2.88 mm, giving a 0.1° angular resolution per pixel; a pixel covers about 0.7 km on the surface of the Earth for an ISS altitude of 400 km. Sampling time is 2.5 μs.

Attached to the Russian MRM-1 module on board the ISS (Fig. 19), the detector will detect UHECRs above 2×10^{19} eV with a yearly exposure of about five times PAO (for $E > 5 \times 10^{19}$, where the K-EUSO response is flat; see Fig. 20). K-EUSO is planned to operate for a minimum of three years and it can function for more than six years if the lifetime of the ISS is extended.

The main goals of K-EUSO are the following:

(1) To perform the first all-sky observation of the UHECR, in order to establish whether—and at what energy—the particle fluxes of the two hemispheres are different.

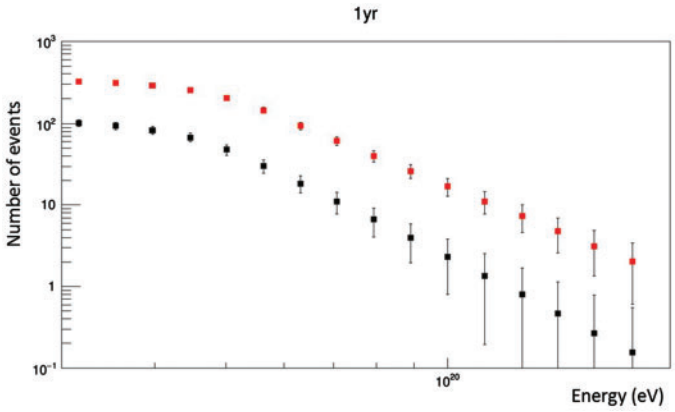

Fig. 21. Integral number spectra as observed on each hemisphere of the whole sky after one year of K-EUSO-Schmidt observation (error bars are statistical errors; Ref. [41]). The red points represent the number of events in the north, based on TA (Ref. [42]), the black points correspond to southern hemisphere events using the PAO spectrum (Ref. [10]).

Northern and southern skies are very asymmetric in the highest-energy region: assuming TA and PAO spectra (Refs. [33,34]), the expected number of K-EUSO (Schmidt optics) events at $E > 57$ EeV is about 140 in the northern hemisphere and 30 in the southern hemisphere after one year of observations, whereas almost the same number of events would be expected in both hemispheres from the isotropic sky. The difference in the number of events arises partially from the overall energy scale difference between TA and PAO.[2] Even after adjusting the relative energy scale, however, the fluxes above $10^{19.5}$ eV significantly differ in both ground experiments. Whether the remaining difference, a large N–S dipole anisotropy, is due to the intrinsic physics or the measurement systematic is one of the very important questions the present ground experiments are facing. The measurement of K-EUSO will give a definite answer to this question after the first six months of operation.

An all-sky measurement will have a lower systematic error in the comparison of the particle fluxes in the two hemispheres. K-EUSO will have to be cross-calibrated with the ground arrays, normalizing the absolute flux in the low-energy range (from $\simeq 3 \times 10^{19}$ eV) to study differences in the spectral shape among the two hemispheres, especially in the highest-energy region. See Fig. 21 for the number of events expected in each hemisphere after three years of observation.

(2) To analyze UHECR clustering to independently confirm (or rule out) the presence of hotspots in the northern and southern hemispheres, and compare their spectral indexes.

K-EUSO's second physics target is independently confirming, or refuting, a TA hotspot at (α, δ) = (146.7°, 43.2°) (Ref. [36]) and a PAO warm spot in the Cen A direction (Ref. [37]). After one year of observation, the TA hotspot will be confirmed at the 3σ level. See Fig. 22 for an example of the simulated sky.

The PAO's warm spot has an angular size of 15° radius in the direction of Cen A, with 14 events including 4.5 background events in a data sample of $E > 58$ EeV and 142 total events. K-EUSO, assuming a signal of the same strength, would obtain a similar number of events in the warm spot in five years of observations.

[2] The spectra of TA and PAO in $10^{18.2}$ eV–$10^{19.5}$ eV coincide well by shifting the energy scale of either experiment by approximately 8.5% (Ref. [35]).

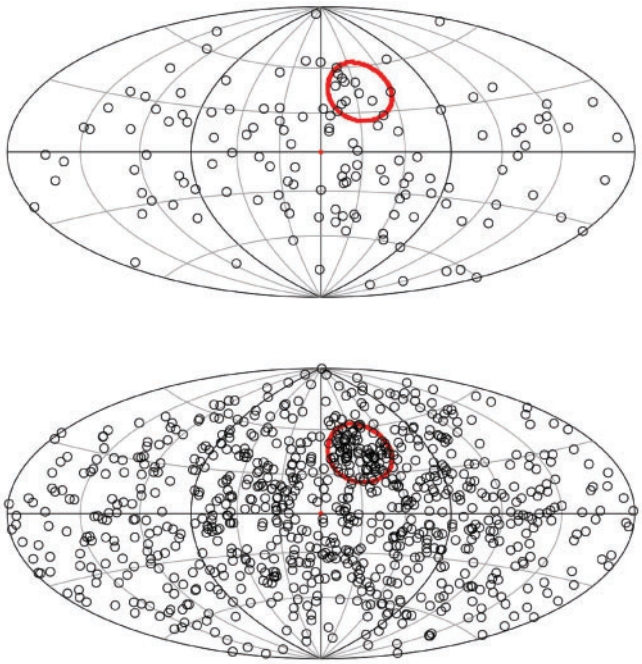

Fig. 22. Top: One of 10^5 simulated random event sets overlaid with the presence of the TA hotspot. After six months of observation, K-EUSO will collect a total of 142 events ($= N_{\rm tot}$) over the whole sky (assuming TA flux), and 15 events ($= N_{\rm on}$) will be in a 20° radius, of which an average of 4.5 events ($N_{\rm bg}$) would be random background. The chance probability is 2.42σ with LEE (look elsewhere effect; Ref. [43]) and 3.36σ without the LEE assumption. Bottom: K-EUSO three-year sky with the TA hotspot. Values are $N_{\rm tot}$=852, $N_{\rm on}$=90, and $N_{\rm bg}$=26.9; 7.5σ with LEE and 7.8σ without LEE are expected. Both maps are in equatorial coordinates.

(3) To study possible UHECR anisotropies over various angular scales, including a possible correlation to nearby large-scale extragalactic structures ($\approx 40°$), Milky Way–related features, and dipole-type anisotropy.

The key to resolving the origin of UHECRs and understanding the mechanisms of acceleration and propagation in extragalactic space lies in the study of their angular distribution and the anisotropy on the celestial sphere. If we are dealing with astrophysical sources, the closest objects should dominate the scene or at least contribute to some anisotropy in the sky. If the sky is mostly isotropic this would strongly favor some kind of cosmological model involving ultra-heavy dark matter and top-down production of UHECR (Ref. [38]).

Given the anisotropy of the nearby ($\simeq 100$ Mpc) universe, diffusive propagation of UHECRs from nearby extragalactic sources would result in a nonzero dipole flux. Furthermore, excesses along a plane, e.g., the super-Galactic one, would be detectable as a quadrupole structure. The result of a joint TA–PAO study for dipole anisotropy (Ref. [39]) (at $E > 10^{19}$ eV) could be confirmed by K-EUSO (above 5.7×10^{19} eV) with much reduced systematics. K-EUSO opens the possibility of anisotropy to study at the highest-energy region, above 57 EeV, and also by combining and unifying the measurements of all experiments to obtain improved statistics. Particles of higher energy are less bent by magnetic fields, and the anisotropy should grow with energy, making the measurement at $E > 5.7 \times 10^{19}$ eV all the more relevant.

(4) Investigate phenomena intrinsic to the Earth's atmosphere or induced by the meteoroids coming from space.

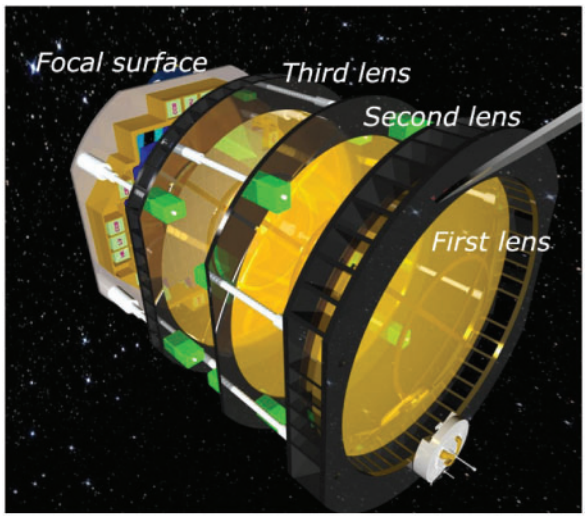

Fig. 23. Model of the JEM-EUSO detector, refractor optics with Dragon launcher configuration. Lens diameter is 2.5 m.

These objectives will be reached after six months of data gathering in flight and significance will be improved after three years of flight (Ref. [40]).

9. JEM-EUSO

The current JEM-EUSO design relies on a Space-X Dragon launcher to be delivered on the ISS. It is a refractor design (Fig. 23), employing three Fresnel lenses to focus the UV light on a 300 k channel focal surface. This new design improves on the original HTV-delivered version. The acceptance of JEM-EUSO is expected to be at least 10 times larger than PAO, allowing a quantitative jump in statistics, and clarification of the origin of the UHECRs. POEMMA, a multimessenger probe for astrophysics, is also under study (Refs. [44,45]).

Acknowledgements

We acknowledge funding from ASI, the Italian Space Agency; MAE, the Ministry of External Affairs; high relevance projects between Italy and Japan. The work is partially supported by a Russian Space Agency and Russian Foundation for Basic Research grant 16-29-13065-ofi-m, KAKENHI (grants-in-aid for scientific research) numbers 16H02426 and 17H02905. We dedicate this paper to Jacek Karczmarczyk and Yoshiya Kawasaki, who passed away in 2016. We thank the referee for the corrections and suggestion, which have greatly improved the paper.

References

[1] R. Benson and J. Linsley, ICRC **8**, 145 (1981).
[2] R. E. Streitmatter, AIP Conf. Proc. **433**, 95 (1998).
[3] Y. Takahashi, AIP Conf. Proc. **433**, 117 (1998).
[4] O. Catalano, S. Giarrusso, G. La Rosa, J. Linsley, M. C. Maccarone, B. Sacco, and L. Scarsi, Nucl. Phys. B **80**, 08 (2000).
[5] O. Catalano, M. C. Maccarone, A. Santangelo, L. Scarsi, and [EUSO Collaboration], EUSO – Extreme Universe Space Observatory, in *Astronomy, Cosmology and Fundamental Physics: Proceedings of the ESO/CERN/ESA Symposium Held in Garching, Germany, 4–7 March 2002, ESO ASTROPHYSICS SYMPOSIA*, eds. P. A. Shaver, L. Dilella, and A. Giménez. Springer-Verlag, 2003, p. 427.
[6] O. Catalano, A. Petrolini, A. Santangelo, L. Scarsi, and [EUSO Collaboration], ICRC **2**, 1081 (2003).

[7] B. A. Khrenov et al., AIP Conf. Proc. **566**, 57 (2001).
[8] B. A. Khrenov, Nucl. Phys. B **113**, 115 (2002).
[9] J. H. Adams et al., [The JEM-EUSO Collaboration] Exp. Astron. **40**, 3 (2015).
[10] I. Valino, PoS **ICRC2015**, 271 (2016).
[11] Y. Takahashi et al., [The Telescope Array Collaboration] AIP Conf. Proc. **1367**, 157 (2011).
[12] J. H. Adams Jr. et al., [The JEM-EUSO Collaboration] Exp. Astron. **40**, 281 (2015).
[13] L. Wiencke and A. Olinto, PoS **ICRC2017**, 1097 (2017).
[14] J. H. Adams Jr. et al., arXiv:1703.04513 [astro-ph.HE] [Search INSPIRE].
[15] M. Ricci, M. Casolino, P. Klimov, and [JEM-EUSO Collaboration], ICRC **34**, 599 (2015).
[16] T. Ebisuzaki et al., Acta Astronaut. **112**, 102 (2015).
[17] G. K. Garipov, M. I. Panasyuk, I. A. Rubinshtein, V. I. Tulupov, B. A. Khrenov, A. V. Shirokov, I. V. Yashin, and H. Salazar, Instrum. Exp. Tech. **49**, 126 (2006).
[18] V. A. Sadovnichy et al., Sol. Syst. Res. **45**, 3 (2011).
[19] M. I. Panasyuk et al., Adv. Space Res. **57**, 835 (2016).
[20] G. K. Garipov et al., J. Geophys. Res. **118**, 370 (2013).
[21] N. N. Vedenkin et al., Soviet J. Exp. Theor. Phys. **113**, 781 (2011).
[22] J. H. Adams Jr. et al., [The JEM-EUSO Collaboration] Exp. Astron. **40**, 239 (2015).
[23] V. Morozenko, P. Klimov, B. Khrenov, G. Garipov, M. Kaznacheeva, M. Panasyuk, S. Svertilov, and R. Holzworth, Geophys. Res. Abstracts **18**, EGU2016–496 (2016).
[24] H. Fukunishi, Y. Takahashi, M. Kubota, K. Sakanoi, U. S. Inan, and W. A. Lyons, Geophys. Res. Lett. **23**, 2157 (1996).
[25] R. K. Said, U. S. Inan, and K. L. Cummins, J. Geophys. Res. **115**, 108 (2010).
[26] P. A. Klimov et al., Proc. 6th Int. TEPA Symp.: Thunderstorms and Elementary Particle Acceleration (TEPA2016) (2017).
[27] P. A. Klimov et al., Bull. Russ. Acad. Sci, Phys. **81**, 407 (2017).
[28] J. H. Adams Jr. et al., [The JEM-EUSO Collaboration] Exp. Astron. **40**, 117 (2015).
[29] J. H. Adams Jr. et al., [The JEM-EUSO Collaboration] Exp. Astron. **40**, 135 (2015).
[30] B. A. Khrenov et al., Phys. Atom. Nucl. **67**, 2058 (2004).
[31] G. K. Garipov, M. Y. Zotov, P. A. Klimov, M. I. Panasyuk, O. A. Saprykin, L. G. Tkachev, S. A. Sharakin, B. A. Khrenov, and I. V. Yashin, Bull. Russ. Acad. Sci, Phys. **79**, 326 (2015).
[32] M. I. Panasyuk et al., J. Phys.: Conf. Ser. **632**, 012097 (2015).
[33] R. U. Abbasi et al., arXiv:1707.04967 [astro-ph.HE] [Search INSPIRE].
[34] A. Aab et al., J. Cosmol. Astropart. Phys. **04**, 038 (2017).
[35] V. Verzi, D. Ivanov, and Y. Tsunesada, arXiv:1705.09111 [astro-ph.HE] [Search INSPIRE].
[36] R. U. Abbasi et al., Astrophys. J. Lett. **790**, L21 (2014).
[37] A. Aab et al., Astrophys. J. **804**, 15 (2015).
[38] A. Addazi and M. Bianchi, J. High Energy Phys. **12**, 89 (2014) [arXiv:1407.2897 [hep-ph]] [Search INSPIRE].
[39] R. U. Abbasi et al., [Telescope Array Collaboration], [arXiv:1511.02103 [astro-ph.HE]] [Search INSPIRE].
[40] T. Ebisuzaki, K-EUSO proposal (2014).
[41] M. Casolino, A. Belov, M. Bertaina, T. Ebisuzaki, M. Fukushima, P. Klimov, M. Panasyuk, P. Picozza, H. Sagawa, Shinozaki K., and [JEM-EUSO Collaboration], PoS, **ICRC2017**, 368 (2017).
[42] D. Ivanov, PoS, **ICRC2015**, 349 (2015).
[43] E. Gross and O. Vitells, Euro. Phys. J. C **70**, 525 (2010).
[44] A. V. Olinto et al., [arXiv:1708.07599 [astro-ph.IM]] [Search INSPIRE].
[45] A. Olinto et al., PoS **ICRC2017**, 542 (2017).